ORIGINAL ARTICLE

Spectroscopic characterization of Brooker's merocyanine in Silicalite-1 and ZSM-5 leading to second harmonic generation

Jennifer S. Holt · Corey Lewandoski ·
Casandra Sheldon

Abstract The use of porous materials has become increasingly significant in the pursuit of novel composite materials with nonlinear optical properties. The microporous channels in Silicalite-1 and ZSM-5, which have identical crystal frameworks but different chemical composition, were used to study the role of zeolite composition on dye adsorption and organization, leading to second-harmonic generation (SHG). The dye molecule, known as Brooker's merocyanine (4-[(1-methyl-4(1H)-pyridinylidene)ethylidene]-2,5-cyclohexadien-1-one), exhibits one of the largest known molecular hyperpolarizabilities for small dye molecules, but it crystallizes centrosymmetrically. When Brooker's merocyanine was adsorbed to Silicalite-1 powder, no SHG was detected, but when adsorbed to ZSM-5, the powder was SHG-active. Spectroscopic characterization of the new materials was used to determine the dye loading in each zeolite. The hydrophilic ZSM-5 channels proved to be essential for dye adsorption and alignment within the channels as compared to the hydrophobic Silicalite-1 which did not appreciably adsorb the dye. The effect of dye protonation and isomerization on adsorption to each zeolite was also studied, with neither having an effect on the amount of dye adsorbed.

Keywords Host–guest chemistry ·
Second harmonic generation · Brooker's merocyanine ·
Zeolites · Dye molecules

J. S. Holt (✉) · C. Lewandoski · C. Sheldon
School of Science, Penn State Erie, The Behrend College,
4205 College Dr., Erie, PA 16563, USA
e-mail: jsh18@psu.edu

Introduction

The study of host–guest materials offers the opportunity to create new materials with a variety of practical applications if the fundamental properties of the resulting material can be controlled and optimized. Specifically, the design of new nonlinear optical materials using host–guest chemistry has become increasingly attractive due to the potential to modify and control the molecular parameters necessary for second harmonic generation (SHG). To generate SHG materials, molecules with large molecular hyperpolarizabilities (β) must by aligned noncentrosymmetrically (lack a center of inversion) to create a large overall second-order susceptibility (χ^2). Host–guest chemistry has great potential to satisfy both conditions by combining a host material that can impart long-range order on highly-polarizable guest molecules. For practical nonlinear optical materials, the resulting material must be optically transparent and resistant to thermal or chemical degradation. It must also be relatively easy to generate. Porous zeolites with embedded dye chromophores have shown great potential because of their unique composite structure which optimizes these characteristics [1]. Zeolites, such as Silicalite-1, are known to be transparent to infrared radiation used for SHG [2] and are very stable in ambient conditions. Early dye-zeolite SHG materials were prepared by inserting *p*-nitroaniline into a variety of zeolites due to the small molecular size and relatively large β value ($\sim 46 \times 10^{-30}$ esu) of the molecule [3]. Cox et al. were the first to report SHG from dipolar chains of *p*-nitroaniline in the acentric ALPO$_4$-5 host [4, 5]. More recently, other dye molecules have been inserted into a variety of zeolite powders and films, as described in a review article by Schulz-Ekloff and coworkers [1]. A variety of techniques to control the insertion of dyes into a specific zeolite

(zeolite L) was summarized by Calzaferri and Lutkouskaya [6]. Further work is still needed, however, to broaden the variety of dye-zeolite materials that exhibit SHG properties.

Merocyanine dyes have been identified as particularly interesting guest candidates for nonlinear optical materials due to their inherently large β values [7]. The guest of interest in this work is Brooker's merocyanine (4-[(1-methyl-4(1H)-pyridinylidene)ethylidene]-2,5-cyclohexadien-1-one), also known as stilbazolium betaine and abbreviated as BM (Fig. 1a). BM has one of the largest known β values for simple chromophores at -1000×10^{-30} esu [8]. It naturally crystallizes in a centrosymmetric alignment with no inherent SHG [9]. The most stable conformation is the planar trans-isomer [10]. Solvent polarity greatly affects the electronic structure of BM, resulting in incredibly large solvatochromic response (maximum absorption wavelength is 620 nm in chloroform and 442 nm in water) [11]. Protonated BM (pKa = 8.57) [12] is known to undergo photoisomerization from the trans to cis isomer, leading to a stable photostationary state that is comprised of both isomers in equilibrium [13]. The deprotonated form, however, does not isomerize. The various forms of BM make it an ideal candidate to probe the effect of dye structure on the ability to enter the zeolite channels.

MFI zeolites have a two-dimensional channel structure that can be used to organize dye molecules within the rigid crystalline host. This zeolite framework consists of straight, slightly elliptical channels (5.2 Å × 5.8 Å) and perpendicular sinusoidal channels (5.4 Å in diameter) [14] (Fig. 1b). Trans-stilbene molecules, which are closely related in size to BM, have been shown to occupy the straight channels rather

than the sinusoidal channels [15]. Figure 1c gives the crystal structure, with the hypothesized location of BM within the channels, if all of the channels were completely filled with dye molecules. Silicalite-1 has Si/Al = ∞, while ZSM-5 may be crystallized with varying Si/Al ratios, which affects the acidity of the zeolite channels [16]. High aluminum content makes the channels more hydrophilic, while the Silicalite-1 channels are hydrophobic.

Recent work has aimed to improve the degree of dye loading, orientation of molecules and inherent β values in the guest chromophore. One of the most promising studies that led to a new, stable SHG material was from the Yoon group, where they incorporated hemicyanine molecules, $\beta \geq 770 \times 10^{-30}$ esu, into Silicalite-1 films [2, 17]. The hydrophobic interactions between the Silicalite-1 channel and an organic tail attached to hemicyanine caused the dye to enter the channels in an aligned fashion. Since a long tail was necessary for ordering (18-carbon chain was optimal), only a few dye molecules could be incorporated into each channel (24 at most) due to the length of the tail and the thickness of the zeolite film (400 nm). Further studies have altered the organic tail group [18] or inserted from the excited state [19] to increase the degree of ordering or the amount of inserted dye.

This work takes a different approach to achieve alignment of a large β-value chromophore. Instead of improving the hydrophobic interactions by altering the dye, the dye will be kept constant and differences in the hydrophobic versus hydrophilic interactions between different zeolites and the BM molecule will be characterized. The compact size of BM, relative to the modified hemicyanine previously studied, offers the potential to incorporate more dye

Fig. 1 The zwitterionic, trans configuration of Brooker's merocyanine (a), a schematic view of the intersecting channel structure of MFI zeolites (b), and an illustration of the crystal structure for both Silicalite-1 and ZSM-5 if BM filled all of the straight channels (c). This is a pictorial representation, not an optimized structure
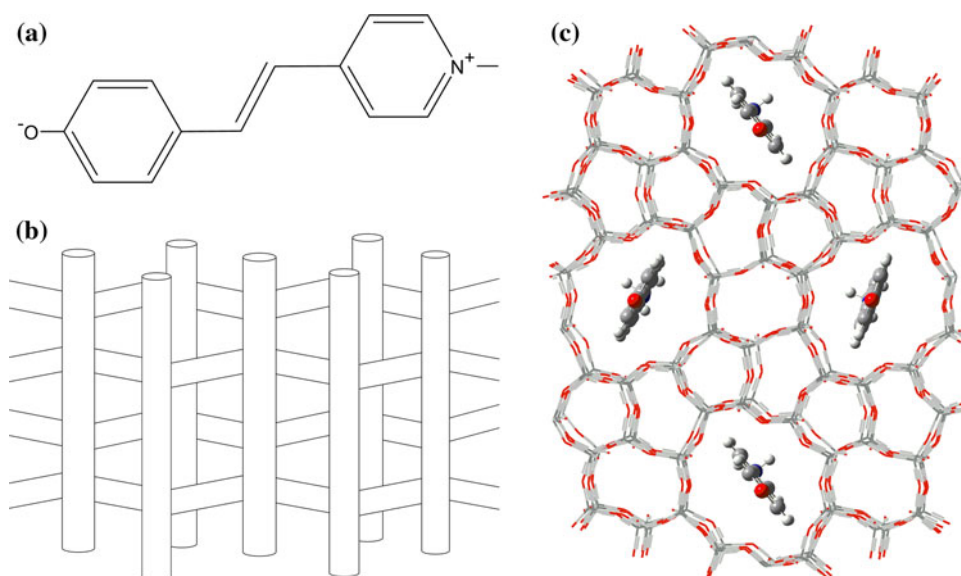
molecules within each channel, and the inherent molecular dipole will aid in alignment. In this work, we will report the amount of dye loading for BM adsorbed to ZSM-5 and Silicalite-1 under different conditions, as well as the spectroscopic characteristics and SHG response of each material. In addition, a simple model will be proposed in order to understand the location of dye molecules in both Silicalite-1 and ZSM-5.

Experimental

Zeolite synthesis and characterization

Silicalite-1 and ZSM-5 were prepared using standard recipes from the International Zeolite Association [20]. Briefly, Silicalite-1 was prepared using Aerosil 130 fumed silica (Degussa), ammonium fluoride (JT Baker) and tetrapropylammonium bromide (Alfa Aesar) as a templating agent (1 SiO_2: 0.08 TPABr: 0.04 NH_4F: 20 H_2O). The resulting gel was hydrothermally treated in a PTFE-lined autoclave at ∼170 °C (±10 °C) for 96 h, followed by microfiltration and calcination at 550 °C overnight. ZSM-5 was prepared by using Silicalite-1 seed crystals prepared from a solution of sodium hydroxide (Fisher Scientific), tetrapropylammonium hydroxide (Aldrich Chemicals) and silicic acid (MP Biomedicals) (0.8 Na_2O: SiO_2: 0.05 TPAOH: 20 H_2O). The solution was stirred for an hour followed by hydrothermal heating at 170 °C for 12–18 h. ZSM-5 gel was prepared by mixing sodium aluminate (Reidel-de Haen), sodium hydroxide, silicic acid and water and aged for an hour (3.25 Na_2O: Al_2O_3: 30 SiO_2: 958 H_2O). The seed crystals were then added and the mixture was aged for another hour before hydrothermal heating at 170 °C for 36 h. The ZSM-5 crystals were isolated and exchanged to H-ZSM-5 through four ammonium nitrate rinses (0.1 M at 60 °C, 150 mL/g zeolite) [21] and subsequently calcined at 550 °C overnight to convert the NH_4^+ to H^+. The size, morphology and composition were confirmed using SEM (Hitachi 570), SEM/EDX (LEO 1450 VP/Apollo 40 SDD), powder x-ray diffraction (Bruker D8 Advance powder X-ray diffractometer), and elemental analysis (Perkin Elmer Optima 5300V, Galbraith Industries), and the results are reported in the Supplementary material 1. Coffin-like Silicalite-1 grains were ∼5 × 7 × 20 μm^3, with a 2 × 2 × 20 μm^3 ledge on the surface due to intergrowths. The rounded ZSM-5 crystals were smaller at 2 × 3 × 7 μm^3, with many more intergrowth regions evident. The ZSM-5 crystals had a Si/Al ∼ 18, as determined by elemental analysis. Finally, BET analysis (Micromeretics ASAP 2020) using N_2 was performed to characterize the zeolites before and after dye adsorption.

Dye loading of zeolites

Dye loading was accomplished using aqueous solutions of Brooker's merocyanine (Aldrich) of varied concentrations. The pH of the dye solution was controlled by the addition of 6.0 M HCl or NaOH in order to affect the protonation of the dye as it approached the zeolite channel. Although a buffered solution would be preferred, the presence of additional ions in solution would compete with dye insertion into the zeolite channels, and was therefore minimized. To ensure the competitive insertion of the sodium ions from the sodium hydroxide did not affect the dye loading, the amount of dye adsorbed using NaOH was compared to insertion from pure water and differences were within the experimental error. Approximately 100 mg of freshly calcined (550 °C, 12 h) zeolite powder was soaked in 10 mL of the dye solution for 3 days with continuous stirring. The powder was collected by microfiltration, air dried after copious rinsing and then soaked in fresh DI water to remove any weakly bound dye. The powders used for the dye loading measurements were then rinsed with ethanol using a Soxhlet extractor, as described by Herance and coworkers [22].

Several methods were used to accurately determine the dye loading of each zeolite. The first method was to determine the difference in the absorption using a Cary 300 UV/Vis spectrometer or in the emission peak heights using a Fluoromax-3 spectrometer of the reference dye solution as compared to the solution after the zeolite was added. All acidic measurements were made after prolonged exposure to ambient lighting so the dye was in the photostationary state. The ZSM-5 solutions were diluted after dye loading had occurred to obtain results within the instrumental limits.

The second method used HF to dissolve the zeolite and measure the amount of dye that had been adsorbed directly. The procedure used was outlined by Kim et al. [18] with the following modifications: 10 mg of dye-loaded zeolite (prepared from a basic solution) was treated with HF, and the resulting solution was neutralized with 1.5 mL of 6.0 M NaOH before dilution to a final volume of 20 mL to ensure the dye was deprotonated and did not photoisomerize. A Beer's Law plot prepared from solutions that mimic the dissolved matrix was used to determine the adsorbed dye concentration of the dye loaded Silicalite-1 and ZSM-5.

### Spectroscopic characterization of BM/zeolite powders

Solid-state spectra were recorded using diffuse reflectance and emission spectroscopy. The diffuse reflectance spectra of the BM adsorbed to zeolite powders were recorded using an integrating sphere (Labsphere) within the Cary 300

spectrometer, with a highly reflective Spectralon reference material. Spectra are reported using an equation derived from the Kubelka–Munk theory, $F(R) = (1 - R)^2/2R$, which gives a direct relationship between dye concentration and the diffuse reflectance (R) of the material [23]. Emission spectra were collected by mounting the powder onto a glass slide using vacuum grease, and positioning the slide at 10–20° from the beam (excitation wavelength = 400 nm). Changes in the BM/ZSM-5 powders over time were observed by comparing the spectra of a fresh sample to annealed samples that were heated at 60 °C for 12 h. One sample was placed in an evacuated cell, while a second sample was placed in a vial with a water saturated vapor.

NLO measurements were obtained using the Kurtz-Perry powder method [24]. A Brilliant B Nd:YAG laser at 1064 nm (peak pulse = 700 mJ, 10 Hz repetition rate) was filtered with a long pass filter. After passing through the sample, a dichroic mirror and 532 nm interference filter, the signal was collected through a fiber optic cable into a monochromator and R928P photomultiplier tube. SHG was measured relative to urea.

Results

The amount of dye adsorbed to each zeolite was quantified using absorbance and fluorescence spectroscopy, and the results are summarized in Table 1. The absorbance spectrum of the dye solution was recorded before and after Silicalite-1 (Fig. 2) and ZSM-5 (Fig. 3) was added to acidic and basic dye solutions. The main absorbance peak shifted from 371 nm for the acidic solution to 442 nm for the basic solution. It should also be noted that the difference in peak heights between the acidic and basic solutions is due to the presence of both cis and trans isomers of BM in the acidic solution. The cis isomer has a smaller extinction coefficient than the trans isomer [14], resulting in lower absorbance values for the same dye concentration. The excitation and emission spectra of the BM solutions were also used to quantify the dye loading. An example of these spectra is shown in Fig. 4 for the acidic solution
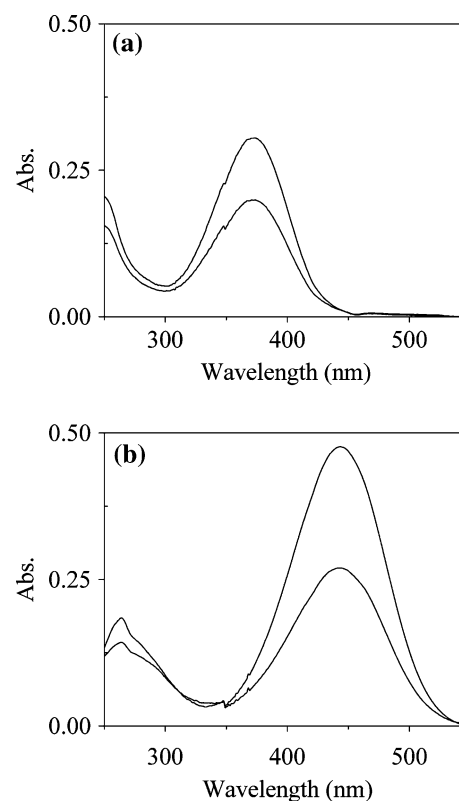
Fig. 2 Absorbance spectra of an aqueous BM solution before (*upper line*) and after addition (*lower line*) of Silicalite-1 powder at pH = 1.9 (**a**) and pH = 12.1 (**b**). The dye concentration was 1.7×10^{-5} M

before and after ZSM-5 addition, with the spectra for the other samples exhibiting similar lineshapes. The only difference in the other samples was that the emission peak shifted from 505 nm (maximum excitation at 380 nm) for the acidic solutions to 575 nm (maximum excitation at 430 nm) for the basic solutions. The difference between dye loading from an acidic solution and a basic solution for each zeolite was within the measurement uncertainties of each method. Finally, these loading results were verified by measuring the amount of BM in the zeolites directly using HF to free the dye from the zeolite. As there was no measureable difference in the solution studies of dye adsorption from either an acidic or basic solution, the HF method was only applied to samples where the dye was

Table 1 Amount of dye adsorbed to Silicalite-1 and ZSM-5 under different pH conditions using absorbance and emission spectra of the dye solution

	Acidic		Basic		HF treatment[a]
	Absorbance	Emission	Absorbance	Emission	
Silicalite-1	2×10^{-7}	2×10^{-7}	4×10^{-7}	5×10^{-7}	2×10^{-7}
ZSM-5	7×10^{-5}	4×10^{-5}	9×10^{-5}	5×10^{-5}	1×10^{-4}

All values are in moles dye/gram zeolite

[a] The amount of dye adsorbed using the HF digestion method on crystals that were initially loaded from a basic solution is also reported
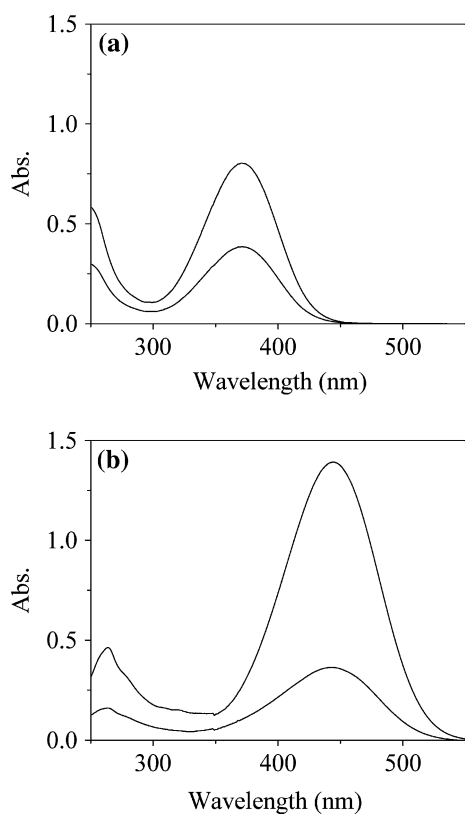
Fig. 3 Absorbance spectra of an aqueous BM solution before (*upper line*) and after addition (*lower line*) of ZSM-5 powder at pH = 1.3 (**a**) and pH = 12.0 (**b**). The dye solution during dye uptake was 1.7×10^{-3} M, but was diluted to 8.5×10^{-5} M for absorbance measurements
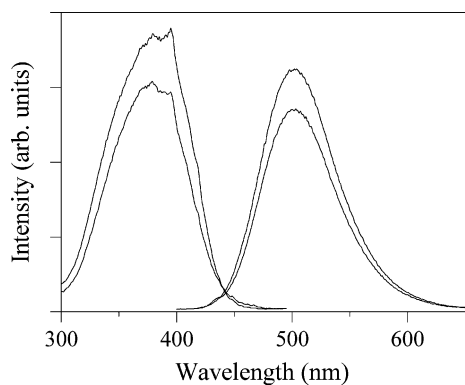

Fig. 4 Fluorescence excitation and emission spectra of an acidic aqueous BM solution before (*upper spectra*) and after addition (*lower spectra*) of ZSM-5 powder. The excitation and emission of a basic BM solution was identical to the acidic solution, except the emission peak was shifted to 575 nm (maximum excitation at 430 nm)

adsorbed from a basic solution for comparison. These results were in good agreement with both acidic and basic solution dye loading values, as shown in Table 1. The ZSM-5 dye adsorption was almost two orders of magnitude larger than the Silicalite-1 uptake, indicating a strong

preference for ZSM-5 over Silicalite-1. The magnitude of dye loading was also similar to those reported for the adsorption of a related dye (4-*N*,*N*-dimethylamino-4′-nitrostilbene) to ZSM-5, which was reported as 5×10^{-5} mol/g [25].

It has been shown that zeolites will maintain a low, constant pH within the zeolite channels, even when the pH of the solution surrounding the zeolite is varied by as many as four pH units [26]. The normalized solid-state diffuse reflectance and emission spectra of the BM/Silicalite-1 and BM/ZSM-5 powders prepared from acidic and basic solutions were very similar, as shown in Fig. 5, indicating the dye became protonated when adsorbed to the zeolite. The solid-state spectra were generally noisier than the solution spectra due to the low dye concentration within the crystals, especially in BM/Silicalite-1. The 25 nm red-shift of the powder diffuse reflectance spectra from the protonated dye in solution is due to changes in solvation and environmental effects imposed by the zeolite channel. The main diffuse reflectance peak for the BM/ZSM-5 powder was broader (FWHM = 6200 cm^{-1}) than the peak for the BM/Silicalite-1 powder (FWHM = 2900 cm^{-1}). Due to
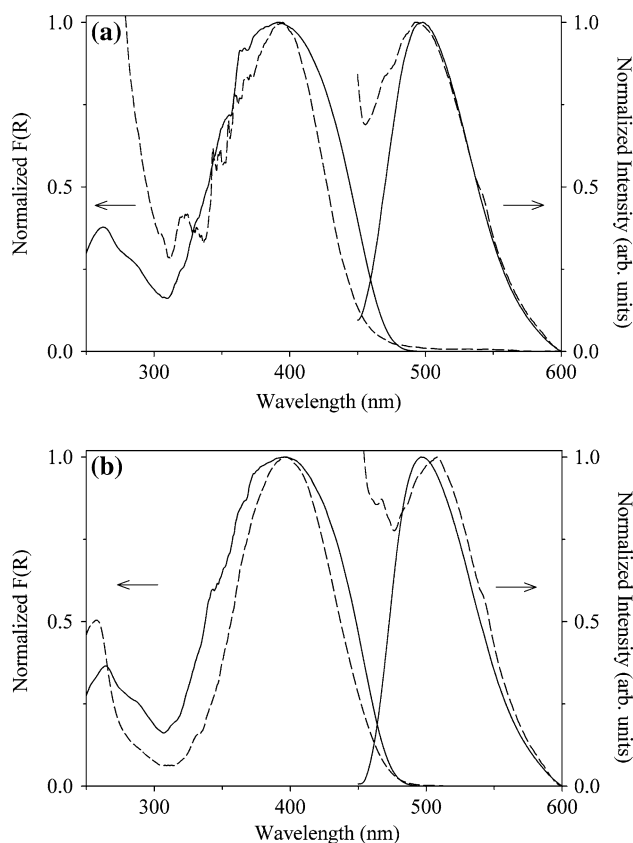
Fig. 5 Normalized solid-state diffuse reflectance (as *F(R)*) and emission spectra for BM adsorbed to Silicalite-1 (*dotted line*) and ZSM-5 (*solid line*) prepared from an acidic solution (**a**) and a basic solution (**b**)

the low dye content of the Silicalite-1 samples, the intensity of the 261 nm reflectance peak was masked by scattering at low wavelengths, and the emission peak could not be completely resolved from the tail of the excitation source. It should be noted that the main reflectance peak position is ideal for SHG from 1064 nm lasers, as the dye is at most weakly absorbing at 532 nm, leading to optical transparency in the region of the spectrum for SHG.

In addition to the solid-state spectra, the SHG response of BM/Silicalite-1 and BM/ZSM-5 powders was monitored. SHG was not detected from the zeolite reference powders or the BM crystals. In addition, SHG was not detected from BM/Silicalite-1. However, the BM/ZSM-5 powder exhibited a measurable SHG signal. The intensity of the signal was 0.22 times the urea SHG signal, a strong SHG powder reference material. When the BM/ZSM-5 powder was stored in ambient conditions, the SHG response was constant over several weeks, but when revisited after several months, there was no measurable SHG activity. To explore possible explanations for the loss of SHG over extended time, an SHG-active BM/ZSM-5 sample was gently annealed in the presence and absence of water vapor to determine if humidity affected the SHG signal. In both cases, the SHG signal decreased to below our detection limit after annealing. The peak shape and position of the diffuse reflectance spectra were identical for each sample, as shown in Fig. 6, although there was a decrease in the peak height of the water-rich annealed sample. The emission spectra were normalized to compare peak widths and were identical. This indicated although the dye concentration decreased upon heating in high humidity, the dye structure was not affected.

In order to further characterize the location of the dye molecules in Silicalite-1 and ZSM-5, the powders were characterized using BET analysis. The surface area and pore volume were determined before and after dye loading using the BET equation and t-plot analysis, and the results are summarized in Table 2. The ZSM-5 powders had slightly less surface area and more mesopores than the Silicalite-1 powder. The mesopores were likely due to cracking or intergrowths, but were less than 5% of the overall surface area, based on the t-plot results. When dye was added, there was a decrease in the BET surface area (and t-plot surface area) for both zeolites. Silicalite-1 dropped by 7.0%, while ZSM-5 decreased by 22%, again indicating preferential adsorption to ZSM-5. The same pattern was observed for the change in pore volume in each zeolite, which confirms that BM enters the ZSM-5 channels in much greater quantity than it enters the Silicalite-1 channels.

A simple spatial model was developed in order to relate the BET results to the dye loading measurements. BM was estimated to be ∼15 Å in length by 5 Å in width, based on
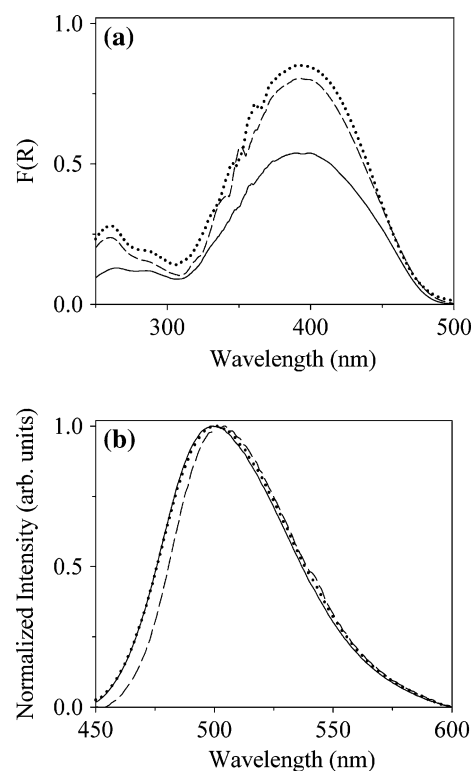
Fig. 6 Solid-state diffuse reflectance (**a**) and emission spectra (**b**) of BM adsorbed to ZSM-5 (*dashed line*) compared to the same material annealed at 60 °C in an evacuated cell (*dotted line*) and in a cell saturated with water vapor (*solid line*). The diffuse reflectance spectra were reported as $F(R)$, while the emission spectra were normalized for comparison

Table 2 BET results of surface area and volume of Silicalite-1 and ZSM-5, as well as the percent decrease in both values due to Brooker's merocyanine adsorption

	BET surface area[a] (m^2/g)	Percent decrease	t-Plot pore volume (cm^3/g)	Percent decrease
Silicalite-1	355	7.04	0.172	4.07
ZSM-5	303	22.4	0.152	22.4

[a] Surface area was determined from the BET plot of the pure zeolite and values for both zeolites were very similar to the t-plot surface area due to micropores

computational modeling. The surface area of each zeolite was estimated by assuming the crystal to be rectangular blocks and using SEM to estimate the crystal size (see Supplementary material 1). The ledges on Silicalite-1 were treated as additional $2 \times 2 \times 20$ μm^3 blocks on the surface of the crystals. The model assumed a unit cell of 2.0×1.3 nm^2 with two channels per unit cell [27]. These zeolites are known to exhibit a complex pattern of intergrowth regions that would hinder the accessibility of some channels, although the exact structure is currently under debate [28] and references therein. For this analysis, it was

Table 3 Results of spatial model used to determine surface coverage versus channel loading

	Minimum dye to cover surface	Maximum dye to cover surface	Maximum dye to fill channels	Average measured dye adsorption
Silicalite-1	1×10^{-6}	3×10^{-6}	8×10^{-4}	3×10^{-7}
ZSM-5	1×10^{-6}	3×10^{-6}	7×10^{-4}	7×10^{-5}

All units are moles dye/gram zeolite

assumed that each channel was accessible in order to determine the maximum possible dye loading. The minimum and maximum number of dye molecules on the surface were determined by assuming that the long axis of the molecule was parallel or perpendicular to the surface, respectively, and are reported in Table 3. A similar model was proposed by Calzaferri et al. [29] for the surface coverage of a related dye on zeolite L crystals, and they found the dye needed to cover the surface was 6×10^{-6} mol/g, which is in good agreement with the current model. The current model was also used to determine the maximum loading to completely fill the channels. As state earlier, trans-stilbene, which is similar in size to BM, was found in the straight channels of ZSM-5 with no evidence of the molecules in the sinusoidal channels [15]. Therefore, the maximum channel loading was determined by filling the longest possible straight channels, which were 7 µm for Silicalite-1 and 3 µm for ZSM-5. The resulting loading values are also reported in Table 3.

Discussion

The attraction of BM molecules to both Silicalite-1 and ZSM-5, as measured by the amount of dye adsorbed, was characterized under different experimental conditions. The dye molecules were strongly bound to the zeolites, as soaking the powders in fresh water or treating with Soxhlet extraction resulted in no measurable difference in dye loading before and after extraction using the HF digestion method. ZSM-5 adsorbed two orders of magnitude more dye molecules than Silicalite-1 as a result of favorable interaction between the dipolar dye molecules with the hydrophilic ZSM-5 channels. Although the chemical composition of the zeolite strongly affected the amount of dye adsorbed, varying the dye structure by varying the pH of the solution did not affect dye adsorption. The protonated dye molecule in the acidic solution can undergo cation exchange, but this resulted in the same amount of dye adsorbed when compared to adsorption of the neutral molecule in a basic solution. In addition, the acidic solution contained both cis and trans BM isomers in a photostationary state, while the basic solution contained only the

trans isomer. Again, the similarity of the amount of dye adsorbed from the acidic and basic solutions indicated that the presence of the cis isomer in solution did not alter the extent of dye adsorption to either zeolite. These studies indicated that the only difference in the amount of dye adsorbed as a result of different experimental conditions was due to the chemical composition of the zeolite channel. The hydrophilic ZSM-5 zeolite (due to the aluminum in the crystal) adsorbed significantly more dye due to the favorable interactions between the hydrophilic channels of ZSM-5 and the inherent dipole of BM.

The location of the dye molecules was also of interest in order to understand the differences between the two zeolite hosts. The amount of dye needed to cover the surface or fill the channels was compared to the average of all dye loading measurements for both zeolites. The actual loading for Silicalite-1 was 3×10^{-7} mol/g, which would be enough to partially coat the surface, based on the spatial model. If all the adsorbed dye went into the Silicalite-1 channels, there would only be 1–2 molecules/channel. In contrast, the average of the dye loading measurements for ZSM-5 was 7×10^{-5} mol/g, which was more than could be accommodated on the surface. This value corresponds to 200 molecules/channel and a 10% decrease in pore volume, which is far less than the predicted maximum loading of 2,000 molecules/channel. As an aside, it should be noted that Fig. 1c is shown with far more dye molecules than would be observed in a cross-section of the actual material. The BET results indicated a 22% decrease in the ZSM-5 pore volume upon dye insertion. The differences may be attributed to coadsorbed water molecules trapped within the channels. In addition, recent studies of ZSM-5 have indicated that dye molecules are not uniformly located throughout the zeolite channels, but are concentrated at the edges of the material [28]. Both of these properties would block the channels, resulting in a larger decrease in pore volume in the BET analysis when compared to the actual loading results.

SHG requires a noncentrosymmetric alignment of hyperpolarizable molecules over a length scale equal to that of the wavelength of light being used. Molecules adsorbed on a surface must lack an inversion center because there can be no mirror plane through the interface boundary. This causes a noncentrosymmetric alignment in at least one direction, which leads to the possibility of SHG from surface adsorption. SHG can also occur as a result of BM alignment within the zeolite channels as a result of how the dye approaches the channel entrance. If SHG resulted from surface adsorption, both zeolites would exhibit nominal SHG. However, BM adsorbed to Silicalite-1 exhibited no SHG. Therefore, it must be the greater concentration and interaction of dye molecules within the channels of ZSM-5 that led to SHG. The inherent dipole of the BM molecules

would affect how the molecules approach and enter the channels by preferentially adsorbing one end of the molecular dipole, which would then influence the insertion of the next dye molecule into that channel. This would lead to alignment within the channels across the scale necessary to observe SHG.

Chemical and thermal stability are required for a practical SHG material. Although the SHG signal from the BM/ZSM-5 material was stable over several weeks, longer periods led to the loss of SHG. One possible explanation was the displacement of dye molecules by water entering the channels. It has been reported that *p*-terphenyl molecules in zeolite L channels were displaced by water over time when exposed to moderate relative humidity at room temperature [30]. The BM/ZSM-5 material exhibited the same behavior, as observed by the decrease in the diffuse reflectance spectra of the moisture-rich sample when compared to the fresh sample (Fig. 6a). However, if the displacement of dye by water caused the loss of SHG, the sample heated in an evacuated, dry cell should remain SHG-active, which was not the case.

Another possible explanation is a slow rearrangement of dye molecules within the channels. This may occur by realignment at the channel intersections, or it may arise from migration of the dye further into the ZSM-5 channels. Recent studies of ZSM-5 have indicated that dye molecules are not uniformly located throughout the zeolite channels, but are concentrated at the edges of the material [31]. Over time, the dye molecules will slowly diffuse further into the channels, leading to the separation of molecules beyond the organized distance needed for SHG. This process would be enhanced by annealing the sample and accounts for the fact that all samples that were heated or aged led to a loss of SHG.

The magnitude of SHG for BM/ZSM-5 (0.22 times urea) was somewhat less than related dye-zeolite materials, such as *p*-nitroaniline in the 1-d channels of AlPO$_4$-5 which has been reported as ∼1.5 times urea when corrected for the difference in reference material [5]. Herance et al. reported the SHG efficiencies for *p*-nitroaniline in this zeolite framework as ∼150 times urea [22]. Although the SHG signal from BM/ZSM-5 was small, the simple fact that SHG was observed is significant and indicates that further optimization should be undertaken in order to achieve results comparable or even larger than current dye/zeolite materials. The use of thin films of zeolites is known to increase the SHG response by an order of magnitude compared to randomly oriented powder [22]. BM can also be adsorbed from the gas phase in order to increase the number of dye molecules in each channel. If the dye loading was increased, diffusion through the channels would decrease and the SHG signal will likely persist. As a

result, BM/ZSM-5 has the potential, based on the results of this initial study, to ultimately lead to a viable SHG material.

Conclusion

This work has shown that the hydrophilicity of the high-aluminum ZSM-5 channel was crucial to the insertion and ordering of BM molecules, leading to the development of a new SHG material. Silicalite-1, a hydrophobic zeolite, exhibited minimal BM dye adsorption and no detectable SHG response. Neither dye protonation nor isomerization affected the loading or ordering of molecules within the channels. The only experimental parameter that resulted in a difference in dye loading was the presence of aluminum in the crystal lattice, leading to 7×10^{-5} mol dye/gram zeolite and a 22% reduction in the pore volume due to dye insertion, as determined from the BET results. The proposed theoretical model predicted a 10% decrease in the pore volume due to the dye loading. The difference in these results could be explained by considering that the channels were blocked, as described earlier. Enough dye was adsorbed in the ZSM-5 crystals to create an SHG-active material. Ultimately, BM inserted into the channels of ZSM-5 was used to develop a new nonlinear optical material and to fundamentally understand of the role zeolite structure and composition plays in guest inclusion and molecular ordering.

References

1. Schulz-Ekloff, G., Wohrle, D., van Duffel, B., Schoonheydt, R.A.: Chromophores in porous silicas and minerals: preparation and optical properties. Microporous Mesoporous Mater. **51**, 91–138 (2002)
2. Shim, T.K., Kim, D., Lee, M.H., Rhee, B.K., Cheong, H.M., Kim, H.S., Yoon, K.B.: Determination of the hyperpolarizability components of hemicyanine dyes by measuring the anisotropic fluorescence and second harmonic of the dyes uniformly aligned within zeolite channels. J. Phys. Chem. B **110**, 16874–16878 (2006)
3. Dulcic, A., Sauteret, C.: The regularities observed in the second order hyperpolarizabilities of variously disubstituted benzenes. J. Chem. Phys. **69**, 3453–3457 (1978)
4. Cox, S.D., Gier, T.E., Stucky, G.D., Bierlein, J.: Inclusion tuning of nonlinear optical materials: switching the SHG of *p*-nitroaniline and 2-methyl-*p*-nitroaniline with molecular sieve hosts. J. Am. Chem. Soc. **110**, 2986–2987 (1988)

5. Cox, S.D., Gier, T.E., Stucky, G.D.: Second harmonic generation by the self-aggregation of organic guests in molecular sieve hosts. Chem. Mater. **2**, 609–619 (1990)

6. Calzaferri, G., Lutkouskaya, K.: Mimicking the antenna system of green plants. Photochem. Photobiol. Sci. **7**, 879–910 (2008)

7. Prasad, P.N., Williams, D.J.: Introduction to Nonlinear Optical Effects in Molecules and Polymers. John Wiley & Sons, Inc., New York (1991)

8. Dulic, A., Flytzanis, C.: A new class of conjugated molecules with large second order polarizability. Opt. Commun. **25**, 402–406 (1978)

9. Jain, K., Crowley, J.I., Hewig, G.H., Cheng, Y.Y., Twieg, R.J.: Optically non-linear organic materials. Opt. Laser Technol. **13**, 297–301 (1981)

10. De Ridder, D.J.A., Heijdenrijk, D., Schenk, H., Dommisse, R.A., Lemiere, G.L., Lepoivre, J.A., Alderweireldt, F.A.: Structure of 4-{2-[1-methyl-4(1H)-pyridylidene] ethylidene}cyclohexa-2, 5-dien-1-one trihydrate. Acta Crystallogr. C Cryst. Struct. Commun. **C46**, 2197–2199 (1990)

11. Catalan, J., Mena, E., Meutermans, W., Elguero, J.: Solvatochromism of a typical merocyanine: stilbazolium betaine and its 2, 6-di-tert-butyl derivative. J. Phys. Chem. **96**, 3615–3621 (1992)

12. Kuder, J.E., Wychick, D.: Acid-base equilibrium in the ground and excited states of a solvatochromic merocyanine dye. Chem. Phys. Lett. **24**, 69–72 (1974)

13. Steiner, U., Abdel-Kader, M.H., Fischer, P., Kramer, H.E.A.: Photochemical cis/trans isomerization of a stilbazolium betaine. A protolytic/photochemical reaction cycle. J. Am. Chem. Soc. **100**, 3190–3197 (1978)

14. Flanigen, E.M., Bennett, J.M., Grose, R.W., Cohen, J.P., Patton, R.L., Kirchner, R.M., Smith, J.V.: Silicalite, a new hydrophobic crystalline silica molecular sieve. Nature **271**, 512–516 (1978)

15. Parise, J.B., Hriljac, J.A., Cox, D.E., Corbin, D.R., Ramamurthy, V.: A high-resolution synchrotron x-ray powder diffraction study of trans-stilbene in zeolite ZSM-5. J. Chem. Soc. Chem. Commun. 226–228 (1993)

16. Ramamurthy, V.: Photochemistry in Organized and Constrained Media. VCH Publishing, New York (1991)

17. Kim, H.S., Lee, S.M., Ha, K., Jung, C., Lee, Y.J., Chun, Y.S., Kim, D., Rhee, B.K., Yoon, K.B.: Aligned inclusion of hemicyanine dyes into silica zeolite films for second harmonic generation. J. Am. Chem. Soc. **126**, 673–682 (2004)

18. Kim, H.S., Sohn, K.W., Jeon, Y., Min, H., Kim, D., Yoon, K.B.: Aligned inclusion of n-propionic acid tethering hemicyanine into silica zeolite film for second harmonic generation. Adv. Mater. **19**, 260–263 (2007)

19. Kim, H.S., Pham, T.T., Yoon, K.B.: Aligned inclusion of dipolar dyes into zeolite channels by inclusion in the excited state. J. Am. Chem. Soc. **130**, 2134–2135 (2008)

20. Robson, H.: Verified Syntheses of Zeolitic Materials. Elsevier, Amsterdam, The Netherlands (2001)

21. Chou, Y.H., Cundy, C.S., Garforth, A.A., Zholobenko, V.L.: Mesoporous ZSM-5 catalysts: preparation, characterization and catalytic properties. Part I: comparison of different synthesis routes. Microporous Mesoporous Mater. **89**, 78–87 (2006)

22. Herance, J.R., Das, D., Marquet, J., Bourdelande, J.L., Garcia, H.: Second harmonic generation of p-nitroaniline incorporated on zeolites: relative efficiencies depending on zeolite structure and film orientation. Chem. Phys. Lett. **395**, 186–189 (2004)

23. Kubelka, P., Munck, F.: Ein beitrag zur optic der fabanstriche. Z. Tech. Phys. **12**, 593–601 (1931)

24. Kurtz, S.K., Perry, T.T.: Powder technique for the evaluation of nonlinear optical materials. J. Appl. Phys. **39**, 3798–3813 (1968)

25. Barbon, A., Bellinazzi, M., Casagrande, M., Storaro, L., Lenarda, M., Brustolon, M.: Photoexcited triplets of dyes in zeolitic nanostructured channels. A time resolved EPR study. Phys. Chem. Chem. Phys. **8**, 5069–5078 (2006)

26. Albuquerque, R.O., Calzaferri, G.: Proton activity inside the channels of zeolite L. Chem. Eur. J. **13**, 8939–8952 (2007)

27. Baerlocher, Ch., Meier, W.M., Olson, D.H.: Atlas of Zeolite Framework Types. Elsevier, New York (2001)

28. Roeffaers, M.B.J., Ameloot, R., Baruah, M., Uji-i, H., Bulut, M., De Cremer, G., Muller, U., Jacobs, P.A., Hofkens, J., Sels, B.F., De Vos, D.E.: Morphology of large ZSM-5 crystals unraveled by fluorescence microscopy. J. Am. Chem. Soc. **130**, 5763–5772 (2008)

29. Calzaferri, G., Bruhwiler, D., Megelski, S., Pfenniger, M., Pauchard, M., Hennessy, B., Maas, H., Devaux, A., Graf, U.: Playing with dye molecules at the inner and outer surface of zeolite L. Solid State Sci. **2**, 421–447 (2000)

30. Devaux, A., Minkowski, C., Calzaferri, G.: Electronic and vibrational properties of fluorenone in the channels of zeolite L. Chem. Eur. J. **10**, 2391–2408 (2004)

31. Nishi, K., Kamiya, N., Yokomori, Y.: Single-crystal structure of a pyridine sorption complex of zeolite HZSM-5 (H-MFI). Microporous Mesoporous Mater. **101**, 83–89 (2007)

32. van Koningsveld, H., Koegler, J.H.: Preparation and structure of crystals of zeolite H-ZSM-5 loaded with p-nitroaniline. Microporous Mater. **9**, 71–81 (1997)